

Visualizing Structural Transitions and Electric Potentials via 4DSTEM

Anuj Pokle^{1,5*}, Andreas Beyer¹, Shamail Ahmed¹, Manveer Singh Munde¹, Damien Heimes¹, Matteo Bianchini², Pascal Hartmann^{2,3}, Torsten Brezesinski², Jürgen Janek^{2,4} and Kerstin Volz¹

¹ Materials Science Center (WZMW) and Department of Physics, Philipps-Universität Marburg, Marburg, Germany.

² Battery and Electrochemistry Laboratory, Institute of Nanotechnology, Karlsruhe Institute of Technology (KIT), Eggenstein-Leopoldshafen, Germany.

³ BASF SE, Ludwigshafen, Germany.

⁴ Institute of Physical Chemistry & Center for Materials Research, Justus-Liebig-University, Giessen, Germany.

⁵ Department of Physics, University of Oslo, Oslo, Norway.

* Corresponding author: anuj.pokle@fys.uio.no

The ability to determine structural and electric potential dynamics at high spatial resolution is critical for understanding energy storage and semiconductor device properties. Scanning transmission electron microscopy (STEM) provides a unique opportunity to perform a large number of different measurements such as imaging, diffraction and spectroscopy simultaneously, down to the sub-atomic dimensions [1]. In this work, we will see the use of a four-dimensional STEM experiment to probe light elements in beam-sensitive energy materials and measure electric fields across GaAs-based p-n junctions.

In recent times the acquisition of four-dimensional datasets, also known as the 4D-STEM technique, has become available using direct electron detectors. The 4D-STEM approach utilizes a fast pixelated sensor acquiring diffraction patterns at each scan point, which allows us to detect structural changes and electric fields at a high spatial resolution. In this topic, we will see the phase transition region using aberration-corrected STEM combined with the pixelated detector (pnCCD). Selecting specific regions in the convergent beam electron diffraction (CBED) patterns and calculating the so-called virtual enhanced ABF (eABF) images is shown to enhance the contrast of the lighter elements even in relatively thicker samples [2].

Another benefit of the pixelated detector is that the angular dependence of the scattered intensity is directly observable, which is of particular importance since any field inside a sample deflects the electron beam. This could be either the longer-ranging electric fields across heterointerfaces or atomic-scale electric fields induced by the Coulomb potentials of the atoms [3], [4]. By combining in-situ biasing with the 4D-STEM technique, we will observe the influence on the depletion region in the GaAs-based p-n junction (refer to Figure 1). Here, the momentum transfer induced by internal electric fields is measured by the diffraction pattern's center-of-mass (COM) shift [5].

This talk aims to expand the developed methodology to full solid-state battery materials. In addition to obtaining the atomic/ electronic structure, chemistry and defect distribution, the projected electrostatic potential can be determined by tracking the phase shift of the electron beam. This will enable us to investigate the role of space-charge models at high-spatial resolutions of the more complex heterointerfaces and grain boundary potentials [6, 7].

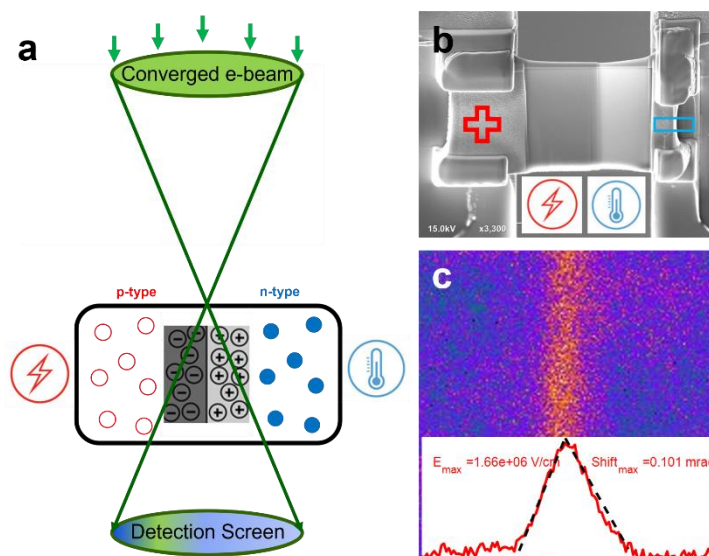


Figure 1: Illustration of a 4D-STEM set up (a) having converged beam passing through a GaAs-based p-n junction model system. The direct electron detector mounted at the bottom can detect COM-shift in milliradian range. (b) shows a Scanning Electron Microscope (SEM) image of a GaAs-based device fabricated on a MEMS chip for in situ experiments. (c) A COM-shift map data acquired by a direct electron detector showing maximum shift angle at the p-n junction, showcasing long-range electric fields.

References:

- [1] C Ophus, *Microsc Microanal* (2019), p. 1. doi: 10.1017/S1431927619000497
- [2] S Ahmed et al., *Advanced Energy Materials* **10**(25) (2020), p. 2001026. doi: 10.1002/aenm.202001026
- [3] N Shibata et al., *Sci Rep* **5** (2015). doi: 10.1038/srep10040.
- [4] JA Hachtel, JC Idrobo and M Chi, *Advanced Structural and Chemical Imaging* **4**(1) (2018). doi: 10.1186/s40679-018-0059-4
- [5] A Beyer et al., *Nano Lett.* (2021). doi: 10.1021/acs.nanolett.0c04544
- [6] C Yang et al., *Nano Lett.* **21**(21) (2021), p. 9138. doi: 10.1021/acs.nanolett.1c02960
- [7] T Bondevik et al., *Phys. Chem. Chem. Phys.* **21**(32) (2019), p. 17662. doi: 10.1039/C9CP02676B